N88-25710

AN ADAPTIVE ARRAY ANTENNA FOR MOBILE SATELLITE COMMUNICATIONS

ROBERT MILNE, Mobile Satellite Project, Communications Canada, Canada.

Communications Canada
Communications Research Centre
3701 Carling Avenue
P.O. Box 11490, Station "H"
Ottawa, Ontario CANADA
K2H 8S2

ABSTRACT

The adaptive array antenna is linearly polarized and consists essentially of a driven $\lambda/4$ monopole surrounded by an array of parasitic elements all mounted on a ground plane of finite size. The parasitic elements are connected to ground via pin diodes. By applying suitable biasing voltages, the desired parasitic elements can be activated and made highly reflective. The directivity and pointing of the antenna beam can be controlled in both the azimuth and elevation planes using high speed digital switching techniques. The design concept, combined with micro-processor technology, provides a powerful mechanism for optimizing the radiation patterns of the antenna under a wide range of operating conditions. The antenna RF losses are neglibible and the maximum gain is close to the theoretical value determined by the effective aperture size. The antenna is compact, has a low profile, is inexpensive to manufacture and can handle high transmitter power.

DESCRIPTION

An antenna consisting of 5 rings of parasitic elements is shown in Fig. 1. It has an angular coverage of 360° in azimuth and between 15° and 60° in elevation. The antenna gain varies between 9 and 11 dBic in the receive band of 1530 - 1560 MHz and between 6 and 10.5 dBic in the transmit band of 1630 - 1660 MHz. The power handling capability is 100 watts. The antenna array, including radome, is less than 2 inches in height and 20 inches in diameter. The parasitic element, shown in Fig. 2, is a composite structure which acts as both radiator and RF choke and incorporates a pin diode and RF by-pass capacitor. The theory of operation is described using the co-ordinate system of Fig. 3. Ignoring the effects of mutual coupling between elements and the finite size of the ground plane, the total radiated field of the array is given by:

$$E(\theta,\phi) = A(\theta,\phi) + KG(\theta,\phi) \sum_{i=1}^{N} \sum_{j=1}^{M(i)} F_{ij}(r_i,\phi_{ij},\theta,\phi)$$

$A(\theta,\phi)$ is the radiated field of the driven element, K is the complex scattering coefficient of the parasitic element, $G(\theta,\phi)$ is the radiated field of the parasitic element, $F_{ij}(r_i,\phi_{ij},\theta,\phi)$ is the complex function relating the amplitude and phases of the driven and parasitic radiated fields. N is the number of rings of parasitic elements, M (i) is the number of elements in the i ring.

By activating the required number of parasitic elements at the appropriate r_i, ϕ_{ij} co-ordinates, the directivity and pointing of the antenna beam can be controlled in both the azimuth and elevation planes.

GAIN

The antenna gain is a function of the array diameter, the number and directivity of the parasitic elements, the frequency of operation, ground plane size and the required angular coverage. Antenna arrays of 3, 4 and 5 rings have been designed, built and tested. The measured gains over the specified angular coverage of 15 - 60° in elevation and 360° in azimuth with the arrays mounted on a 36 inch diameter ground plane are as follows:

No. of Rings:	3	4	5
Rx Gain (dBic)	7.5 - 9.5	8.5 - 10.0	9.0 - 11.0
Tx Gain (dBic)	6.0 - 9.5	6.0 - 10.0	6.0 - 10.5

The measured received gain of a 5 ring array versus elevation angle is shown in Table 1.

RADIATION PATTERNS

To provide coverage between 15° and 60° in elevation 3 beams are required. A maximum of 32 beams are required to provide 360° coverage in azimuth. Typical azimuth and elevation patterns are shown in Figures 4-8. The patterns have been optimized to maximize received gain and inter-satellite isolation and minimize the effects of multipath on communications and tracking performance.

RETURN LOSS

The return loss of the antenna is a function of both frequency and the array switching configuration. The return loss versus frequency for the 3 basic elevation switching configurations is shown in Figure 9. The maximum return loss for all beam positions is less than -12 dB (VSWR <1.7) in both the receive and transmit frequency bands.

RF LOSS/NOISE TEMPERATURE

The RF loss of the antenna is less than 0.1 dB which contributes about 7° K to the systems noise temperature. Noise temperatures of less than 85° K have been measured at the output of the antenna, mounted on a vehicle in a typical operational environment, with the beam pointing at 25° elevation. The noise temperature contribution should be significantly lower at higher elevation angles. The resulting systems G/T will be 1.5 to 2.0 dB higher than conventional phased array designs with higher RF loss but the same net gain.

VEHICLE INTERFACE/EFFECTIVE GROUND PLANE SIZE

The vehicle structure will affect the gain, polarization and radiation patterns of any antenna mounted on it. This is particularly true of an antenna designed for low elevation coverage. Measurements have been conducted using a 5 ring array to determine the effects of ground plane sizes ranging from 4 feet x 5 feet to 10 feet x 5 feet for both flat and curved surfaces, with curvatures of 6°/foot. The effect of extending or curving the ground plane is to tilt the "low" beam towards the horizon, thereby increasing the gain at low elevation angles. A gain of 8 dBic can be achieved at 5° elevation with the array mounted on a 5 feet x 5 feet ground plane.

INTER-SATELLITE ISOLATION

The isolation achievable is a function of antenna directivity, satellite location and the latitude and longitude of the vehicle. Isolation measurements have been carried out using a 5 ring array in an anechoic chamber. The results are shown in Table 2 for various satellite separations and vehicle locations in the U.S. and Canada. Full duplex operation is assumed and that the land vehicle uses the satellite with the higher elevation angle. A ±5° pointing error results in a spread of isolation values. Higher values of isolation can be achieved in some cases at the expense of some loss in antenna gain.

Multipath effects will, however, determine the upper limit of isolation achievable. With the antenna beam pointing at one satellite, signals will be scattered by objects in the beam in the direction of the other satellite. The magnitude of the signals will depend on the proximity and reflecting properties of the scatterers, the relative satellite elevation and azimuth angles, and the directivity of the land vehicle antenna.

CONTROLLER DESIGN

The controller is required to accurately point the antenna beam at the satellite under all dynamic conditions of the host vehicle if the advantages of a directive antenna are to be realized. In the acquisition mode the beam is sequentially stepped through 360° and the beam with the strongest signal selected. The satellite is subsequently tracked by periodically switching the beam on either side of the previous satellite position and selecting the beam with the strongest signal. Successful field trials were conducted in an INMARSAT operational satellite system. The selected circuit time constants were based on a C/N ratio of 50 dB-Hz, a receiver output bandwidth of 1000 Hz and a S/N ratio at the input of the controller of 20 dB. After frequency locking it required less than 20 ms to re-acquire the satellite. The tracking sampling interval was less than 5 ms. The tracking sampling rate could be varied manually from 0.25 Hz to 4 Hz to match vehicle angular velocity.

COST

The predicted cost of the antenna and controller is less than $1000 (Can.) in quantities of 10,000/year. The low cost is due to the elegant simplicity of design. The parasitic element has a minimum number of parts and lends itself to mass production techniques. Its electrical characteristics are highly repeatable and simple to measure, thereby reducing testing and assembly cost. The antenna ground plane provides a well defined interface between the RF and digital switching components and eliminates the need for expensive microstrip.

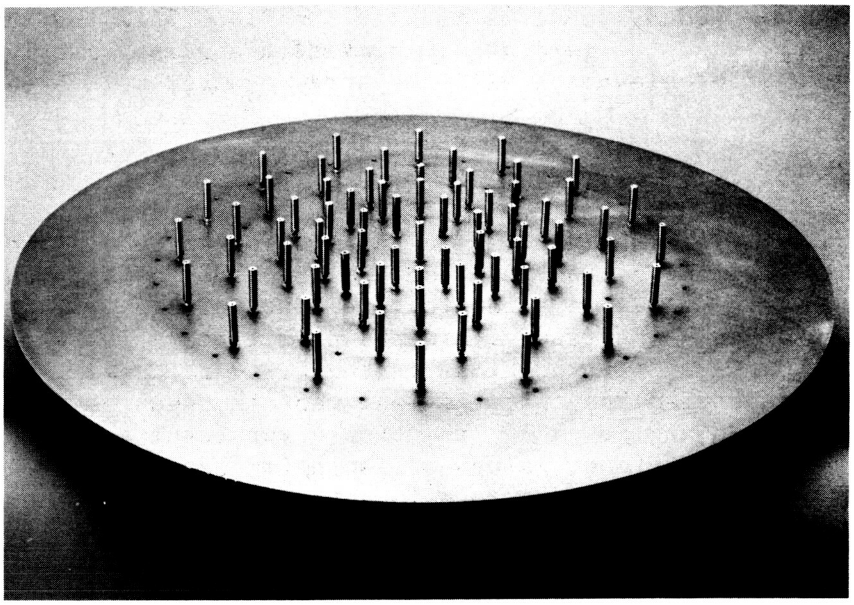

FIG. 1 ADAPTIVE ARRAY ANTENNA

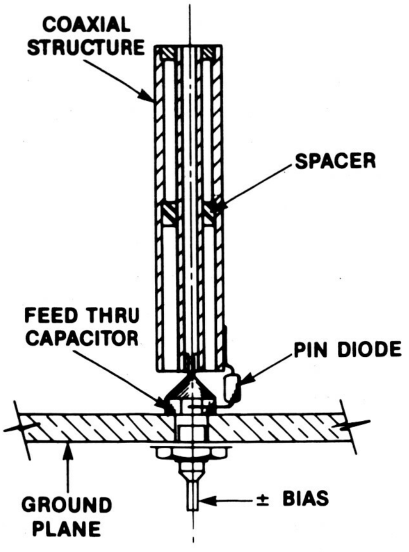

FIG. 2 PARASITIC ELEMENT

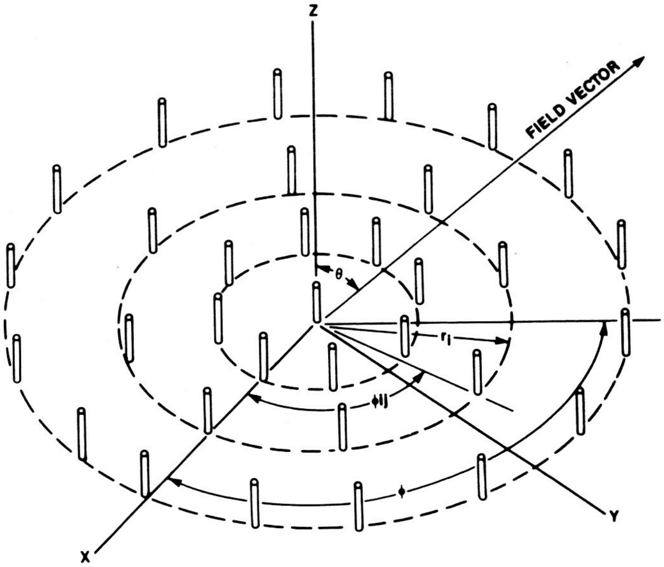

FIG. 3 CO-ORDINATE SYSTEM

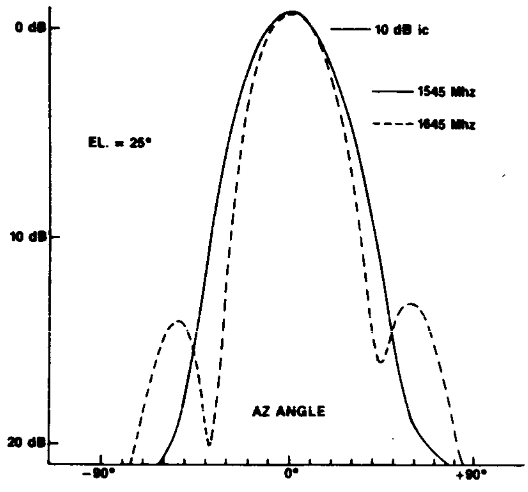

FIG. 4 AZ. PATTERN - LOW BEAM

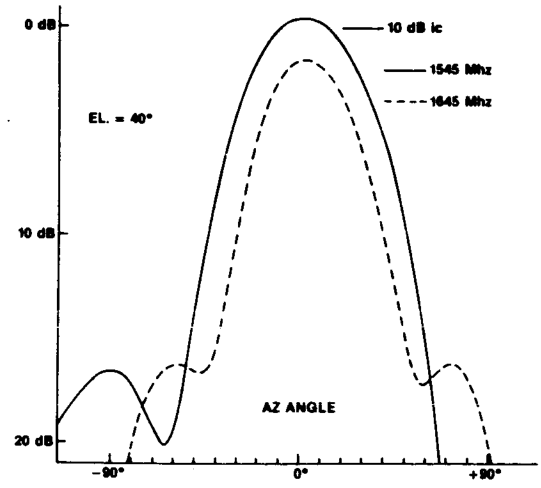

FIG. 5 AZ. PATTERN - INTERMEDIATE BEAM

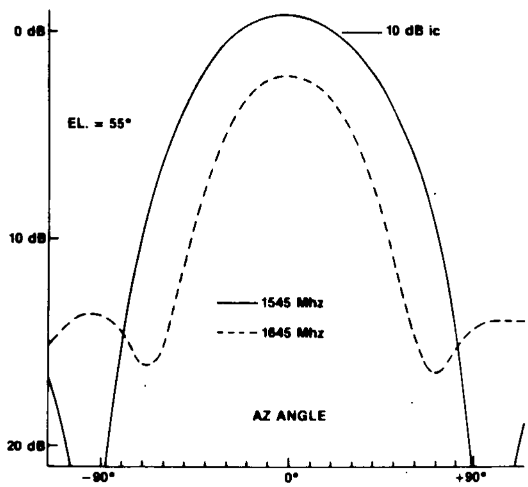

FIG. 6 AZ. PATTERN - HIGH BEAM

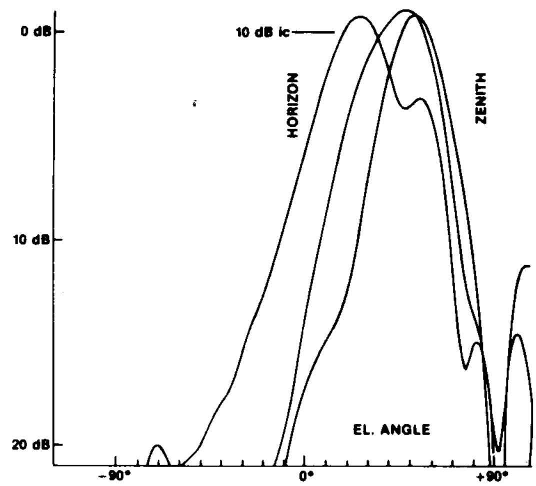

FIG. 7 EL. PATTERNS - 1545Mhz.

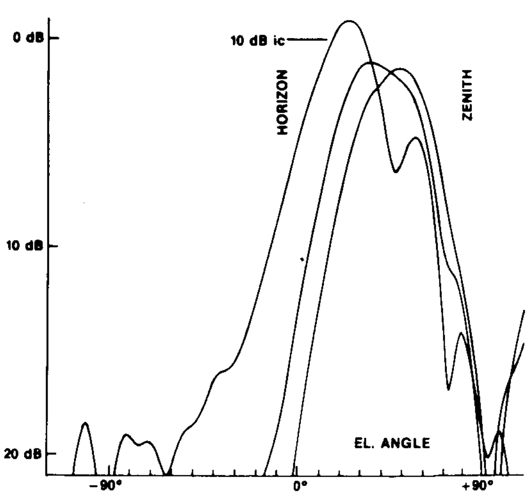

FIG. 8 EL. PATTERNS - 1645Mhz.

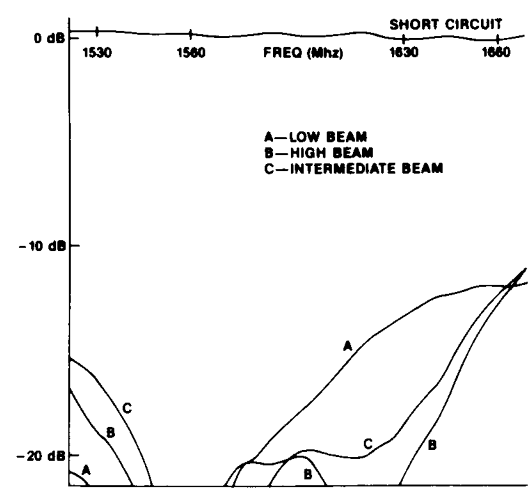

FIG. 9 RETURN LOSS VERSUS FREQUENCY

ELEVATION ANGLE	LOW BEAM	INTERMEDIATE BEAM	HIGH BEAM
0	4.0	-2.6	-9.0
5	6.0	0.0	-6.8
10	7.5	1.8	-4.6
15	9.0	3.9	-2.0
20	10.0	5.7	0.2
25	10.4	7.3	2.7
30	10.4	8.5	4.9
35	9.6	9.6	6.9
40	8.1	10.0	8.4
45	5.8	10.1	9.7
50	4.3	9.9	10.4
55	4.5	8.6	10.4
60	4.6	6.7	9.6
65	3.2	3.7	7.7
70	-0.6	-0.6	5.2

TABLE 1 Measured Rx Antenna Gain (dbic)

Satellite Location	80, 115 (West)		80, 120 (West)		80, 125 (West)		80, 130 (West)	
Frequency	Rx	Tx	Rx	Tx	Rx	Tx	Rx	Tx
Ottawa	9-13	13-20	12-17	18-22	15-20	21-22	18-21	20-23
St. Johns	8-13	9-16	11-16	12-19	15-19	16-19	18-22	20-19
Vancouver	8-13	10-17	11-15	15-16	14-17	15-17	17-19	14-16
Winnipeg	10-15	14-16	13-17	13-15	15-18	13-14	17-19	13-15
Whitehorse	10-14	11-18	12-16	15-20	15-19	19-20	17-19	19-20
Frobisher	10-14	14-19	13-17	16-20	16-20	18-19	19-22	18-20
Inuvik	10-14	11-18	13-17	15-19	14-19	18-19	17-20	18-19
Honolulu	13-14	11-13	14-15	12-15	14-15	13-17	14-16	13-18
Miami	7-10	15-30	11-15	20-27	13-18	24-25	16-20	28-30
New Orleans	8-12	18-25	11-15	24-37	16-22	20-27	19-26	21-24
Los Angeles	10-15	13-18	14-18	17-18	18-20	18-19	20-21	18-21
Salt Lake City	9-15	15-20	13-18	19-20	16-20	19-20	19-22	19-22
Chicago	9-14	15-19	13-18	19-20	16-19	19-20	18-19	19-20
Boston	9-13	11-20	12-16	16-23	15-19	20-22	17-21	21-25
Anchorage	12-16	12-18	13-18	15-19	16-20	18-19	19-22	18-19

TABLE 2 ISOLATION (db) AS A FUNCTION OF SATELLITE LOCATION